THE JOURNAL OF BIOLOGICAL CHEMISTRY
Vol. 280, No. 34, Issue of August 26, pp. 30120–30128, 2005
Printed in U.S.A.

Loss of the von Hippel Lindau Tumor Suppressor Disrupts Iron Homeostasis in Renal Carcinoma Cells*

Received for publication, January 26, 2005, and in revised form, June 27, 2005
Published, JBC Papers in Press, June 28, 2005, DOI 10.1074/jbc.M500971200

Alessandra Alberghini‡§, Stefania Recalcati‡§, Lorenza Tacchini‡, Paolo Santambrogio¶, Alessandro Campanella¶, and Gaetano Cairo‡‖**

From the ‡Institute of General Pathology, University of Milan, Via Mangiagalli 31, 20133 Milan and the ¶Protein Engineering Unit, Dibit, Scientific Institute of Recovery and Care, Saint Raffaele Hospital, Via Olgettina 58, 20132 Milan, Italy, and Internal Medicine 3, Ospedale Maggiore Policlinico, Milano, Italy

Given the modulation of iron metabolism by hypoxia and the high iron requirement of neoplastic cells, we investigated iron metabolism in a human renal cancer cell line with a mutated von Hippel Lindau (VHL) tumor suppressor gene (RCC10) and in a transfectant clone with wild-type VHL (RCC63). The loss of VHL strongly up-regulated transferrin receptor expression in RCC10 cells as a result of hypoxia inducible factor-1 (HIF-1)-mediated transcriptional activation, leading to an increased uptake of transferrin-bound ^{55}Fe. Increased iron availability did not compromise the resistance of VHL-defective cells to oxidative stress or promote faster cell multiplication. Surprisingly, the content of ferritin H and L subunits and ferritin mRNA levels were considerably lower in the RCC10 than in the RCC63 cells. Despite the similarities between HIF-1 and iron regulatory protein 2 (IRP2), we found no evidence of specific regulation of IRP2 by VHL. However, both IRP2 and IRP1 were slightly activated in RCC10 cells, thus indicating that this cell line has a somewhat reduced labile iron pool (LIP). The finding that RCC10 cells had a lower ferritin content but more ferritin-associated ^{55}Fe than RCC63 explains why VHL-lacking cells may have a smaller LIP despite increased iron uptake. We also found a correlation between cytoprotection from iron-mediated damage and efficient incorporation into ferritin of both transferrin and non-transferrin-bound ^{55}Fe. This study shows that, like oncogene activation, the loss of an oncosuppressor rearranges the expression pattern of the genes of iron metabolism to increase iron availability. However, in the case of VHL loss, mechanisms affecting iron handling by ferritin somehow counteract the effects that the reduced content of this protective protein may have on proliferation and oxidant sensitivity.

Iron is an important cofactor needed for a number of essential cell functions, including cell growth (1). Cells need iron to proliferate mainly because ribonucleotide reductase, the rate-limiting enzyme for DNA synthesis, is strictly iron-dependent, but recent evidence has suggested that other components of the cell division machinery, such as cyclin and cyclin-dependent kinases, require iron (2). Consequently, iron chelators have anti-proliferative effects as they lead iron-depleted cells to G_1/S arrest and apoptosis (2). However, iron can also be dangerous as a catalyst of free radical reactions, because it can convert normally produced reactive oxygen species-like molecules formed by cellular metabolic activity into more potent hydroxyl radicals (3). Accordingly, intracellular iron homeostasis is tightly regulated by the reciprocal expression of ferritin, a shell-shaped protein consisting of 24 subunits of two types that can safely store excess iron (4), and transferrin receptor (TfR),[1] which mediates iron entry into the cell. Although transcriptional regulation has been described, the concerted expression of ferritin and TfR is mainly controlled at post-transcriptional level by means of the action of iron regulatory proteins (IRP1 and IRP2), cytoplasmic proteins that bind iron-responsive elements (IRE) in the untranslated regions of TfR and ferritin mRNAs in response to variations in iron levels in the so-called labile iron pool (LIP) (5, 6). When activated, the IRPs enhance TfR mRNA stability and block ferritin mRNA translation, thus facilitating iron uptake over sequestration and generating a pool of iron for cellular metabolic use. Conversely, the down-modulation of IRP activity permits efficient ferritin synthesis and reduces TfR expression, thus preventing potentially toxic iron accumulation. The activity of IRP1 is regulated by interconversion between the RNA-binding form and a form endowed with a 4Fe-4S cluster that possesses aconitase enzymatic activity, whereas IRP2 activity is controlled at the level of protein stability, as it undergoes degradation by the proteasome in response to iron (5, 6).

Given its importance for cell multiplication and its pro-oxidant capacity, iron could be a relevant factor in cancer development. In addition, understanding misregulations of iron metabolism in cancer cells may be important for improving chelation-based therapeutic strategies specifically targeted against tumor cells (7). Information about specific changes affecting iron metabolism in tumors is rather scant, but there have been recent reports of alterations in the genes controlling intracellular iron concentrations, which may facilitate cell proliferation. For example, it has been shown that overexpression of the c-*myc* oncogene down-modulates H ferritin transcription while inducing the expression of IRP2, the cytoplasmic repressor of ferritin mRNA translation. It has therefore been hypothesized that this mechanism, which impairs ferritin synthesis at

* This work was supported by grants from the Italian Association for Cancer Research, Ministero dell'Istruzione, dell'Università e della Ricerca (Fondo per gli Investimenti della Ricerca di Base and Cofinanziamento 2001 and 2002) (to G. C.). The costs of publication of this article were defrayed in part by the payment of page charges. This article must therefore be hereby marked "*advertisement*" in accordance with 18 U.S.C. Section 1734 solely to indicate this fact.

§ Both authors contributed equally to this work.
‖ To whom correspondence should be addressed. Tel.: 39-025-031-5350; Fax: 39-025-031-5338; E-mail: gaetano.cairo@unimi.it.

[1] The abbreviations used are: TfR, transferrin receptor; RCC, renal clear cell carcinoma; IRP1, -2, iron regulatory proteins 1 and 2; VHL, von Hippel Lindau; HIF, hypoxia-inducible factor; LIP, labile iron pool; BSO, buthionine sulfoximine; DFO, desferrioxamine; MTT, 3-(4,5-dimethylthiazol-2yl)-2,5-diphenyltetrazolium bromide; FAC, ferric ammonium citrate; HRE, hypoxia-responsive element; IRE, iron-responsive elements.

two different molecular levels, may be a means of increasing iron availability and useful for cell growth (8).

Like oncogene activation, the lack of an oncosuppressor may also affect iron metabolism in tumors. In particular, we hypothesized that iron homeostasis could be disrupted by the absence of the von Hippel Lindau (VHL) tumor suppressor gene product, a component of the ubiquitin E3 ligase complex that targets the hypoxia-inducible factor (HIF-1α) to proteasome degradation (9). In cells lacking protein VHL, the increased stabilization of the normally unstable HIF-1α leads to overproduction of hypoxia-inducible genes whose action is believed to facilitate tumor growth in adverse microenvironments, invasion, and angiogenesis (10–13). Because iron is a cofactor required by the hydroxylases involved in HIF-1α degradation, the interaction of iron metabolism with VHL may be of interest in relation to the physiology of HIF-1 regulation and alterations of the system in cancer (11).

Iron metabolism is modulated by hypoxia (6), and we and others have demonstrated an HIF-1-dependent transcriptional activation of TfR expression in hepatoma cells exposed to hypoxia (14, 15) and iron chelation (16). Therefore, the aim of the present study was to analyze the expression of TfR and iron-related genes, as well as other parameters of iron metabolism, in a human renal clear cell carcinoma (RCC) cell line that bears an inactivating mutation of the VHL gene (RCC10) and in a clone in which the wild-type VHL gene has been reintroduced by means of stable transfection (RCC63) (17). We found that the lack of VHL caused a profound rearrangement of iron homeostasis, not only activating TfR expression in a HIF-1-dependent manner and inhibiting ferritin expression at mRNA and protein level, but also modifying iron trafficking with preferential iron storage in ferritin that counterbalanced the enhanced TfR-mediated uptake.

MATERIALS AND METHODS

Cell Culture—The human parental VHL-negative RCC10 cell line and a clone derived by means of the stable transfection of VHL (RCC63) (17) were kindly provided by Dr. Karl Plate (Goethe University, Frankfurt, Germany) and were maintained in Dulbecco's modified Eagle's medium supplemented with 10% heat-inactivated fetal calf serum, 2 mM glutamine, 100 units/ml penicillin, and 0.1 ng/ml streptomycin at 37 °C in 5% CO_2. For the RCC63 cells, G418 sulfate (Promega, Milano, Italy, 1 mg/ml) was added to the medium. The embryonic rat heart-derived cell line H9c2 was obtained from The American Type Culture Collection (CRL 1446) and grown as described previously (18). When appropriate, near confluent cells were treated for 24 h with 100 μM ferric ammonium citrate (FAC), 100 μM desferrioxamine (DFO) or 100 μM $CoCl_2$, 1 μM human holotransferrin (all from Sigma).

Transient Transfection Assay—Subconfluent RCC cells were transiently co-transfected using FuGENE (Roche Applied Science) with 1 μg of a 50:1 mixture of the constructs containing fragments of the TfR promoter and the pRL-SV40 reporter vector containing *Renilla* luciferase, which was used to normalize transfection efficiency. The vectors used were pTfRB-luc, which contained a 455-bp fragment of the human TfR promoter region cloned in front of the luciferase gene in the pGL2 vector (Promega, Milano, Italy), pTfRBm-luc in which the bases TACGT in the putative HRE sequence 5′-TACGTGC-3′ were replaced with AATTC (14), and pGL3PGK6TKp containing a HRE multimer (19) (a kind gift of Dr. P. J. Ratcliffe). All of the constructs were verified by DNA sequencing. After 48 h, the cells were collected, washed, and lysed using the reporter lysis buffer (Promega). Luciferase activities were then measured in a Promega luminometer using the Dual-Luciferase Reporter Assay System (Promega) according to the manufacturer's instructions.

Immunoblot Analysis—For the detection of IRPs and ferritin H subunit, the cells were homogenized in Munro buffer (10 mM Hepes, pH 7.6, 3 mM $MgCl_2$, 40 mM KCl, 5% glycerol, 0.2% Nonidet P-40, and protease inhibitors), and the lysates were centrifuged at 800 × *g* for 5 min. To detect TfR, the cells were homogenized in 20 mM Tris-HCl, pH 8, 200 mM LiCl, 1 mM EDTA plus 0.5% Nonidet P-40, and protease inhibitors, and the lysate was kept on ice for 40 min and then centrifuged at 16.000 × *g* for 5 min. HIF-1α was determined in nuclear extracts prepared according to a previous study (20). Aliquots of supernatants containing equal amounts of proteins were electrophoresed in acrylamide-SDS gels and electroblotted to Hybond membranes (Amersham Biosciences). For ferritin H subunit analysis, extracts were resolved by means of non-denaturing PAGE (21). After assessing transfer by means of Ponceau S staining, the membranes were saturated in 4 mM Tris-HCl, pH 7.6, 30 mM NaCl (Tris-buffered saline) containing 20% nonfat milk and 0.1% Tween 80, and incubated with rabbit antiserum to IRP2 (raised against a conserved sequence in the degradation domain of IRP2, 1:100 dilution) (18), rabbit antiserum to IRP1 (1:500 dilution) (22), monoclonal antibody against ferritin H subunit (rH02, 1:5000 dilution), anti-VHL monoclonal antibody (Ig32 BD Pharmingen, 2 μg/ml), monoclonal antibody against human TfR (Zymed Laboratories Inc., 1:1000 dilution), monoclonal anti-human HIF-1α antibody (H1α67, Novus Biologicals, 1:1000 dilution), and a monoclonal antibody to β-actin (Sigma) to control equal protein loading. After incubation with the appropriate secondary antibodies and extensive washing with Tris-buffered saline containing Tween 80, the antigens were detected by chemiluminescence using an immunodetection kit (ECL Plus, Amersham Biosciences) according to the manufacturer's instructions and quantitated by laser densitometry.

RNA-Protein Gel Retardation Assay—The cells were homogenized in Munro buffer; after the addition of dithiothreitol to a 1 mM final concentration, the lysate was centrifuged at 16,000 × *g* for 5 min at 4 °C. Equal amounts of supernatant proteins were incubated with a molar excess of the IRE probe transcribed from the linearized pSPT-fer plasmid containing the IRE of the human ferritin H chain using T7 RNA polymerase in the presence of [α-^{32}P]UTP, and sequentially treated with RNase T1 and heparin as previously described (21). For the supershift experiments, the lysates were incubated with saturating amounts of mouse antiserum raised against recombinant human IRP1 (23) for 10 min at room temperature before being incubated with the IRE probe. After separation on 6% non-denaturing polyacrylamide gels, the RNA-protein complexes were visualized by autoradiography and quantitated by direct nuclear counting using an InstantImager (Packard Instruments Co.).

Determination of Aconitase Activity—Aconitase activity was determined spectrophotometrically at 240 nm, as described before (22), by monitoring the disappearance of *cis*-aconitate. The incubation (1 ml of final volume) contained lysates (100 μg of protein) and 0.1 mM *cis*-aconitate in 0.3 M NaCl (pH 7.0), 37 °C; 1 milliunit is defined as the amount of enzyme that consumed 1 nmol of *cis*-aconitate/min.

Northern Blot Analysis—Total cell RNA was isolated as described (24), and equal amounts were electrophoresed under denaturing conditions. To confirm that each lane contained equal amounts of total RNA, the ribosomal RNA content in each lane was estimated in the ethidium bromide-stained gels by laser densitometry. RNA was transferred to Hybond-N filters (Amersham Biosciences) that were hybridized with the following ^{32}P-labeled DNA probes: human ferritin H and L subunit cDNAs (25), human TfR cDNA (24), H3 histone (26), and the expressed sequence tag clone IMAGp956G0635Q24 encoding human IRP2 (RZPD Berlin, Germany). Quantitative determination was made by direct nuclear counting using an InstantImager (Packard Instruments Co.), and the values were calculated after normalization to the amount of ribosomal RNA.

Determination of Ferritin Subunit Content—Ferritin concentrations were determined in cell lysates by means of an enzyme-linked immunosorbent assay based on monoclonal antibodies specific for human H and L ferritin subunits (rH02 and LF03) and calibrated with the corresponding recombinant homopolymers (27). The specificity and absence of cross-reactivity of the antibodies have been previously described. The microtiter plates were coated with 1 μg of a monoclonal antibody specific for H or L ferritin. Soluble tissue homogenates or standard ferritins were diluted in 50 mM sodium phosphate (pH 7.4), 150 mM NaCl, 0.05% (v/v) Tween 20, 1% bovine serum albumin, and added to the plates. The presence of ferritin was revealed by incubation with the same antibody labeled with horseradish peroxidase. Peroxidase activity was developed with *o*-phenylenediamine dihydrochloride (Sigma). Protein content was measured using the Bio-Rad protein assay kit.

Uptake of ^{55}Fe-Transferrin and ^{55}Fe-FAC—To evaluate the incorporation of ^{55}Fe-transferrin (Tf), the RCC cells were incubated for 30 min at 37 °C in serum-free Dulbecco's modified Eagle's medium plus 0.5% bovine serum albumin to remove cell-bound endogenous Tf. The cells were then washed once with cold phosphate-buffered saline and incubated for 24 h at 37 °C in the same medium containing 1 μM ^{55}Fe-Tf. To label Tf with iron, ^{55}Fe iron citrate was first prepared by mixing $^{55}FeCl_3$

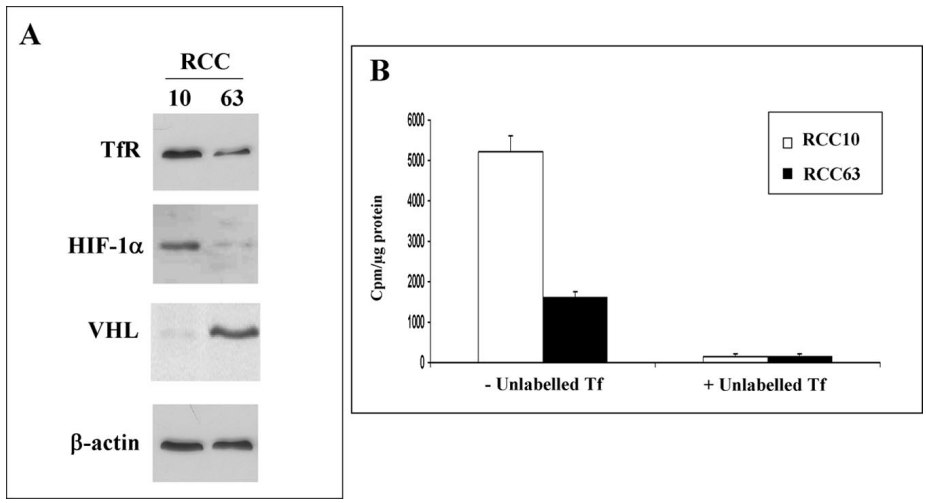

FIG. 1. **Loss of VHL activates TfR expression and transferrin bound iron uptake.** *A*, immunoblot analysis: equal amounts of proteins from lysates of RCC10 and RCC63 cells were loaded onto SDS-polyacrylamide gels and immunoblotted with antibodies against TfR, HIF-1α, and VHL. The blots were reprobed with an antibody against β-actin as a loading control. Antigens were visualized by chemiluminescence. The result shown is representative of three independent experiments. *B*, ^{55}Fe incorporation: RCC cells were incubated in serum-free medium plus 0.5% bovine serum albumin for 30 min. After washing, the cells were exposed to ^{55}Fe-transferrin (Tf) for 24 h in the same medium, in the absence or presence of a 100-fold excess of unlabeled Tf. The cells were then washed and homogenized as described under "Materials and Methods." Cellular iron uptake is expressed as radioactive iron in total homogenates. Mean values ± S.D. of three separate experiments.

(PerkinElmer Life Sciences) with citric acid in a 1:2 molar ratio. Human apo-Tf (Sigma) was incubated with ^{55}Fe iron citrate in a buffer consisting of 0.1 M Tris-HCl, pH 8.0, 10 μM Na_2CO_3 for 1 h at room temperature followed by removal of unincorporated ^{55}Fe iron on YM 30 Centricon filter devices (Millipore). Preliminary experiments showed that this concentration of ^{55}Fe-Tf was enough to allow linear iron incorporation under these conditions. Moreover, no significant incorporation of radioactivity was found when the cells were incubated at 4 °C (data not shown). To evaluate the incorporation of ^{55}Fe-FAC, the cells were exposed for 24 h to 2 μCi/ml ^{55}Fe-FAC prepared as described previously (28) in the presence of 0.2 mM ascorbic acid. When appropriate, the cells were extensively washed with phosphate-buffered saline and further incubated for 24 or 48 h in serum-free medium plus 0.5% bovine serum albumin. At the end of the incubations, the medium was removed and saved, and the cells were washed three times with cold phosphate-buffered saline and homogenized in the Munro lysis buffer used for the immunoblot analysis (see above). Aliquots of lysates were taken to measure the amount of cellular ^{55}Fe uptake by means of liquid scintillation counting with Ultima Gold (Packard Instruments) and protein determination. The homogenates were then centrifuged at 16,000 × *g* at 4 °C for 5 min, and the supernatants were taken for analysis of ferritin by autoradiography or immunoblotting.

Analysis of ^{55}Fe-labeled Ferritin—To evaluate ^{55}Fe iron incorporation into ferritin, equal amounts of proteins prepared from cell lysates incubated with ^{55}Fe-Tf or ^{55}Fe-FAC were analyzed by means of nondenaturing PAGE followed by autoradiography and IstantImager counting (18).

Analysis of Cell Growth and Cytotoxicity—To evaluate cell proliferation, viable cells were counted using thiazolyl blue (MTT, Sigma) as an indicator of mitochondrial function. Briefly, RCC cells (10^5 cells per well) were seeded in quadruplicate in 24-well cell culture plates in the presence or in the absence of 1 μM Fe-Tf; at the indicated time points, the MTT solution was added for 2–3 h, the formazan crystals were dissolved according to the manufacturer's instructions, and the spectrophotometric absorbance was read at 570 nm with the background absorbance at 690 nm being subtracted.

To monitor cytotoxicity, the cells were left untreated or exposed for 24 h to increasing concentrations of FAC or buthionine sulfoximine (BSO) (Sigma); the latter treatment was performed in the presence or in the absence of 1 μM Fe-Tf. At the end of the treatments, cell viability was measured by the MTT assay (18) as described above.

Statistical Analysis—Values are expressed as means ± S.D. The significance of differences was evaluated with the *t* test using the Stat View 4.0 program (Abacus Concept Inc., Berkeley, CA).

RESULTS

Loss of VHL Activates TfR Expression and Iron Accumulation—Given our previous demonstration that TfR is a hypoxia-inducible gene (14), we investigated whether the absence of VHL influences TfR expression by using VHL-deficient RCC10 cells and the RCC63 clone stably transfected with wild-type human VHL (17). Immunoblot analysis of cell lysates normalized for actin content showed that the expression of TfR protein is more than three times higher in RCC10 cells (Fig. 1*A*). In agreement with previous evidence (17), HIF-1α, which was barely detectable in RCC63 cells as a consequence of the forced expression of functional protein VHL, was clearly evident in RCC10 cells which lack VHL, thus demonstrating actual deregulation of the major VHL target (Fig. 1*A*).

To determine whether the higher TfR expression also enhanced iron uptake, the cells were exposed to ^{55}Fe-labeled transferrin, and the total cell content of radioactive iron was determined by means of liquid scintillation counting. The ^{55}Fe content was >3-fold greater in the RCC10 cells, thus indicating that the enhanced levels of TfR are functionally involved in favoring greater iron availability (Fig. 1*B*). Competition by a 100-fold excess of unlabeled transferrin effectively blocked iron incorporation.

Role of HIF-1 in TfR Induction—To understand the molecular basis of the higher TfR expression, we analyzed TfR mRNA levels. In agreement with the results provided by immunoblotting, Northern blot analysis showed a marked difference in steady-state TfR mRNA levels, with a 3-fold higher expression in RCC10 cells (Fig. 2*A*). To assess the role of HIF-1-mediated transcriptional regulation in the induction of TfR expression in VHL-defective RCC10 cells, the two RCC cell lines were transiently transfected with a luciferase reporter gene under the control of a 455-bp fragment of the human TfR promoter (wild-type or mutated in the hypoxia-responsive element, HRE) (Fig. 2*B*); this fragment has been previously demonstrated to be sufficient for the efficient transcription of a reporter gene (14). In line with our previous demonstration that TfR is activated by HIF-1 (14, 16) and the considerable difference in HIF-1 activity in the two cell lines, we found that the wild-type construct was transcribed three times more efficiently in the RCC10 than in the RCC63 cells, whereas no difference was found in the expression of the empty pGL2 basic vector. Importantly, the mutation in the HRE almost completely abolished the differences in transcription, thus demonstrating that the high level of TfR expression in RCC10 cells is caused by HIF-1-mediated transcriptional activation (Fig. 2*C*). Further evidence of the role of HIF-1 was provided by the greatly different expression of luciferase driven by a HRE multimer. When RCC63 cells were exposed to the hypoxia mimetic $CoCl_2$, luciferase expression driven by the TfR promoter reached levels similar to those observed in RCC10 cells, in which expression was not significantly modified by the treatment (Fig. 2*D*).

Increased Iron Accumulation Does Not Promote Oxidative Damage or Cell Proliferation—We next wondered what might

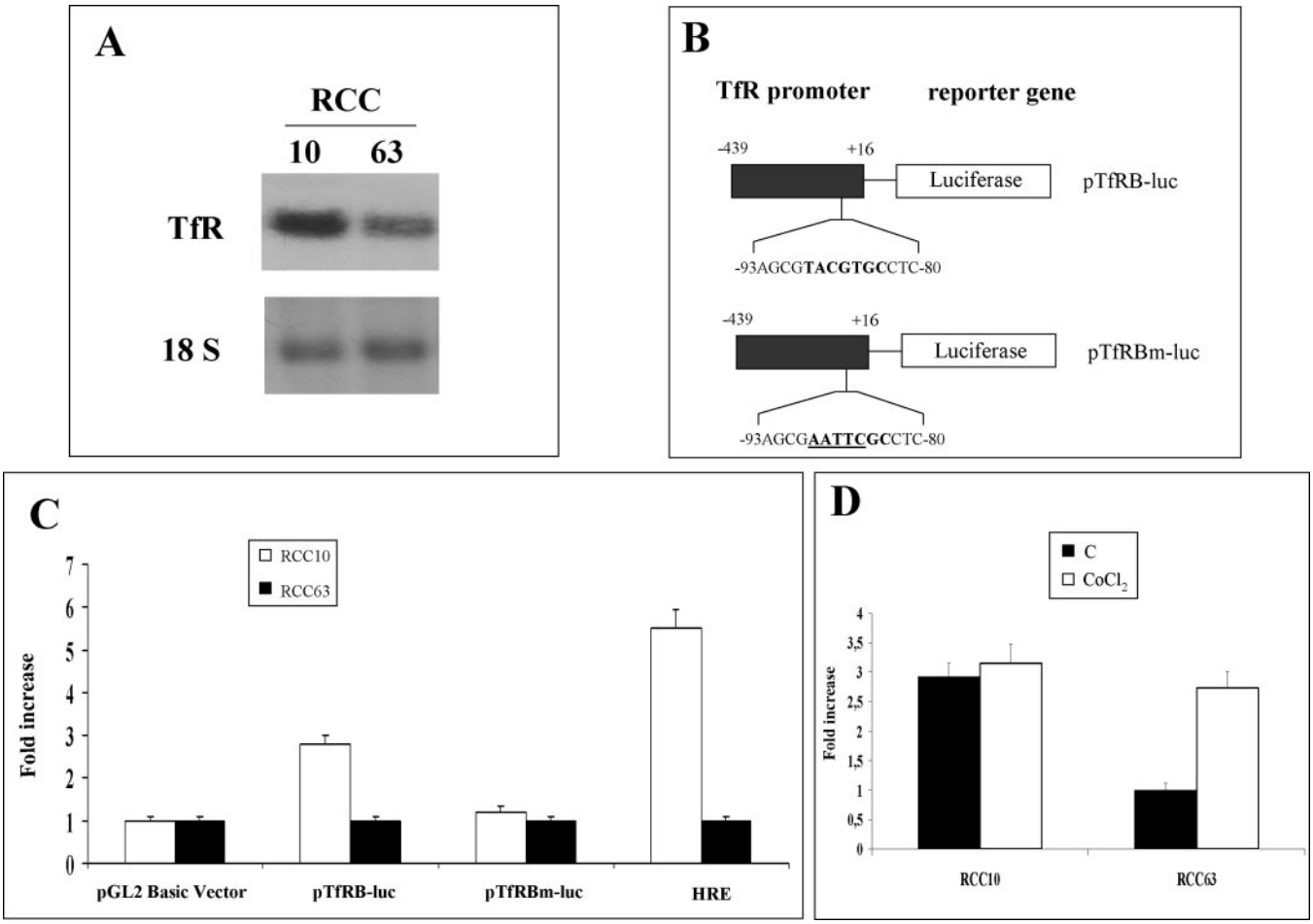

FIG. 2. **Loss of VHL activates HIF-1-dependent TfR transcription.** *A*, Northern blot analysis: a filter with equal amounts of total RNA (as revealed by the ethidium bromide fluorescence of ribosomal RNA) was hybridized with human TfR cDNA. The autoradiogram is representative of three independent experiments. *B*, structure of the TfR constructs used in the transfection experiments. The reporter plasmids contained a 455-bp fragment of the human TfR promoter in front of the firefly luciferase gene; the sequence containing the wild type (pTfRB-luc) or mutated (pTfRBm-luc) HRE (in *bold*) is shown expanded. The HRE core motif, mutated in pTfRBm-Luc, is *underlined*. *C*, transient expression assay: RCC10 and RCC63 cells were transiently transfected with the empty pGL2 Basic vector, or with the reporter plasmids shown in *panel A* and with a construct in which luciferase is controlled by a HRE multimer. The cells were co-transfected with a control vector containing the *Renilla* luciferase gene. Luciferase activity was determined after 24 h, corrected for transfection efficiency according to *Renilla* luciferase activity, and normalized to the activity in RCC63 cells, arbitrarily defined as 1. Mean values ± S.D. of three independent experiments. *D*, transient expression assay: RCC10 and RCC63 cells were transiently transfected with the pTfRB-luc plasmid and with a control vector containing the *Renilla* luciferase gene. After an incubation of 24 h in the absence or in the presence of 100 μM $CoCl_2$, luciferase activity was determined, corrected for transfection efficiency according to *Renilla* luciferase activity, and normalized to the activity in untreated RCC63 cells, arbitrarily defined as 1. Mean values ± S.D. of three independent experiments.

be the consequences of this marked increased of iron content. Given the role of iron in promoting reactive oxygen species formation, we investigated whether RCC10 cells were more prone to undergo oxidative damage. To assess resistance to oxidative stress, the cells were exposed to the glutathione-depleting agent BSO, and their viability was monitored by MTT assay. Fig. 3*A* shows that the susceptibility to BSO of the two RCC cell lines was similar both in the presence and in the absence of the same concentration of diferric transferrin (1 μM) used in the iron incorporation experiments. This suggested that no excess iron remained available to promote free radical reactions. Similar results were obtained when the RCC cells were exposed to increasing concentrations of H_2O_2 (results not shown). On the contrary, an overload of iron (given as ferric ammonium citrate, FAC) greatly enhanced the susceptibility of H9c2 cardiomyocytes to BSO, thus showing that this assay is able to detect the presence of an excess of reactive iron (Fig. 3*B*). The high iron requirements of proliferating cells led us to suppose that the larger amount of iron entering RCC10 cells (which have lost a growth-suppressor gene) was used to promote faster multiplication rate, and so we compared the growth profiles of the two cell lines. As it has been shown that the presence of VHL affects cell multiplication when cells grow to confluence (29), we limited our analysis to subconfluent cells: *i.e.* the same cell density as that used for all of the other determinations made in this study. The measurement of viable cells by MTT assay showed no significant difference in growth rate, with a doubling time of 29 h for RCC10 and 32 h for RCC63 cells (Fig. 3*C*). In agreement with this finding, the mRNA levels of histone H3, whose expression is directly related to the fraction of cells in the S phase of the cell cycle (26), were similar in the two RCC cell lines in the exponential growth phase (Fig. 3*C*, *inset*). Addition of 1 μM diferric transferrin did not significantly affect the cell proliferation of the two cell lines. These results, which are in line with those of several previous studies showing that monolayer growth is not affected by VHL (30), suggest that RCC10 cells do not use the greater availability of iron delivered by transferrin to sustain an accelerated growth rate.

Loss of VHL Down-regulates Ferritin Content—The above results did not explain the fate of the increased amount of transferrin-bound iron entering RCC10 cells and prompted us

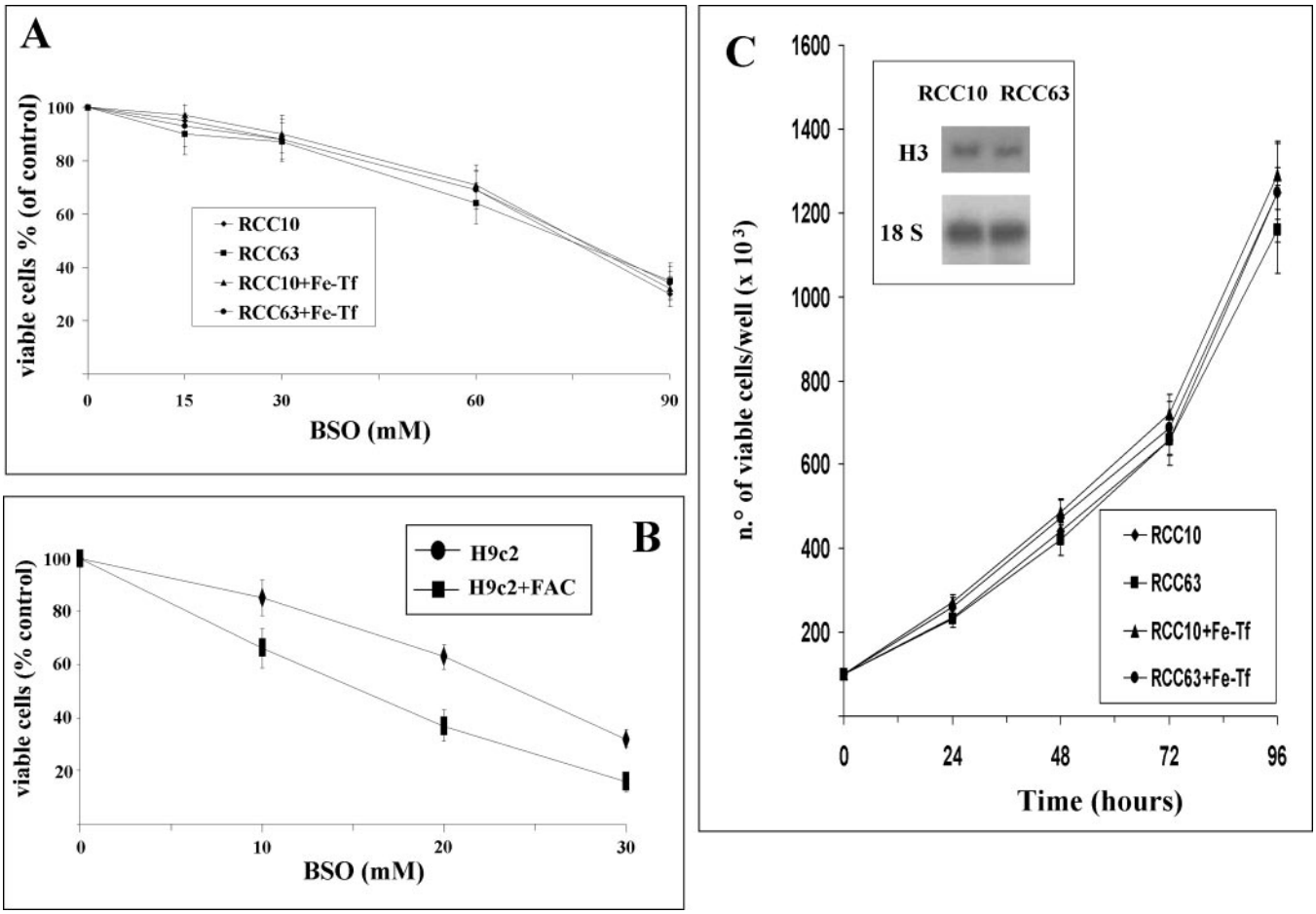

FIG. 3. **Loss of VHL does not affect the response to oxidative stress or growth rate.** *A*, effect of VHL on the toxicity induced by glutathione depletion. RCC10 and RCC63 cells were left untreated or exposed to increasing concentrations of buthionine sulfoximine (*BSO*) for 24 h in the presence or in the absence of 1 μM diferric transferrin (*FeTf*). Toxicity was evaluated as the percentage of viable cells measured by MTT assay, an indicator of mitochondrial function. Mean values ± S.D. of three experiments. *B*, effect of iron on the toxicity induced by glutathione depletion in cardiomyocytes. H9c2 cells were left untreated or exposed to increasing concentrations of BSO for 24 h in the presence or in the absence of 100 μM FAC. Toxicity was evaluated as the percentage of viable cells measured by MTT assay. Mean values ± S.D. of three experiments. *C*, effect of VHL on cell proliferation. The cells were seeded in quadruplicate both in the presence and in the absence of added 1 μM diferric transferrin and their growth was evaluated by MTT assay at different times after seeding. Mean values ± S.D. of four independent experiments. *Inset*, Northern blot analysis of H3 histone mRNA. A filter with equal amounts of total RNA (as revealed by the ethidium bromide fluorescence of ribosomal RNA) from RCC cells grown in the absence of added 1 μM diferric transferrin was hybridized with a probe for H3 histone. The autoradiogram is representative of three independent experiments.

to investigate ferritin expression, because the induction of this iron storage protein is the hallmark effect of the metal (4). Surprisingly, the ferritin H and L subunit levels determined by means of a specific enzyme-linked immunosorbent assay were remarkably lower (85 and 76% reduction, respectively) in the RCC10 cells (Table I). In both cell lines, isoferritins are mainly composed of the H subunit, but the different extent of reduction also shifted the ratio of the two subunits in favor of the L subunit in RCC10 cells. Iron-dependent regulation was maintained in both cell lines, because we found the expected modulation of both ferritin subunits after exposure to an iron load (FAC) or the iron chelator DFO.

Molecular Mechanisms Underlying Down-modulation of Ferritin Expression—We next tried to understand the molecular mechanisms underlying the surprising reduction in ferritin content in VHL-defective cells despite their enhanced iron accumulation. We hypothesized that it be determined at post-transcriptional level by an abnormal stabilization of IRP2 caused by the absence of VHL. IRP2, which plays a predominant role in the regulation of ferritin expression (31–33), might be a target of VHL, because it shares a remarkable number of features with HIF-1, such as inducibility by iron deficiency and hypoxia, fast turnover, proteasome-mediated degradation, and the involvement of 2-oxoglutarate-dependent oxygenases in degradation (34–36). We therefore determined whether the presence and modulation of IRP2 were different in the two cell lines. Immunoblots of cell lysates showed that IRP2 protein levels were slightly higher (1.5-fold) in RCC10 cells, a more modest difference than that obtained by the exposure of RCC63 cells to the iron chelator DFO (Fig. 4*A*). Importantly, IRP2 content was down-regulated by exposure to iron also in the VHL-free RCC10 cells. In agreement with evidence showing that alterations in IRP1 activity occur without changes in the amount of protein (5, 6), IRP1 levels were similar in all the samples (Fig. 4*A*). Although IRP2 is mainly controlled at the level of protein stability, it has been shown that, in some cases, its transcription may be regulated (8, 37); we therefore analyzed IRP2 gene expression, but found no significant differences in IRP2 mRNA levels between the two cell lines (Fig. 4*B*). Taken together, these results suggest that the strong effect of VHL on ferritin expression was not exerted at the post-transcriptional level through direct interaction with IRP2. This was further indicated by experiments in which we measured the RNA-binding activity of IRPs and the enzymatic activity of aconitase, the cluster-less form of IRP1. As human IRP1 and IRP2 comigrate, RNA bandshift assays showed that the com-

TABLE I
Ferritin H and L subunit content

The amounts of H and L chains in the RCC10 and RCC63 cell extracts were determined by enzyme-linked immunosorbent assay using monoclonal antibodies against the corresponding recombinant human ferritin subunits. When indicated, cells were exposed to FAC or DFO for 24 h. Values are mean ± S.D. of four determinations.

	L ferritin content	H ferritin content	H/L ratio
	ng/mg of protein		
RCC10	54.2 ± 6.1[a]	91.8 ± 9.6[a]	1.7
RCC10 plus FAC	162.8 ± 14.2[b]	340.4 ± 19.7[b]	2.1
RCC10 plus DFO	33.1 ± 2.2[b]	53.3 ± 4.2[b]	1.6
RCC63	226.7 ± 11.3	611.7 ± 16.2	2.7
RCC63 plus FAC	678.8 ± 52.3[b]	1836.4 ± 69.2[b]	2.7
RCC63 plus DFO	135.6 ± 18.1[b]	262.7 ± 14.5[b]	1.9

[a] $p < 0.001$ *versus* RCC63.
[b] $p < 0.001$ *versus* the respective untreated cell line.

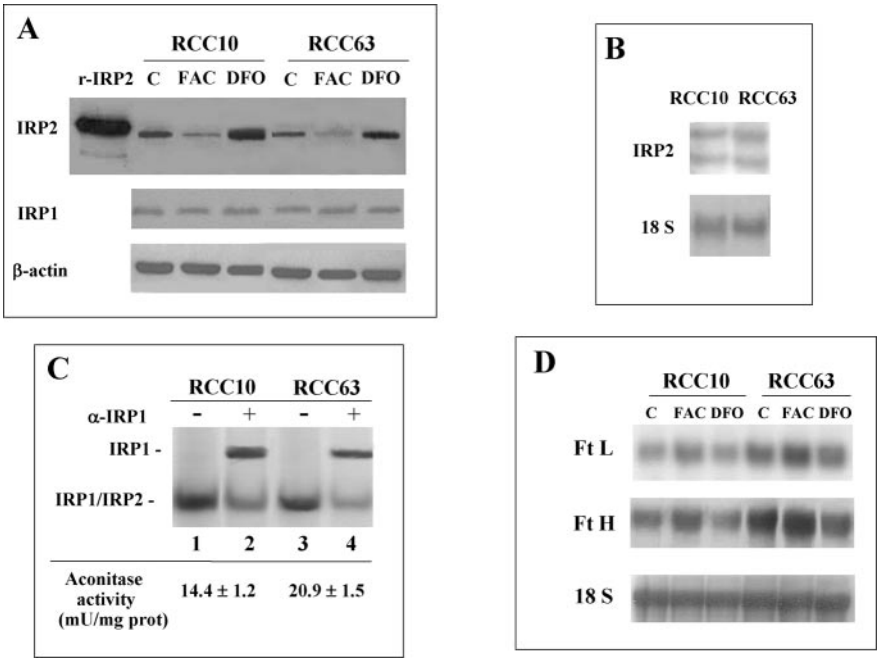

FIG. 4. **Mechanisms of reduced ferritin expression in VHL-deficient cells.** *A*, immunoblot analysis: equal amounts of proteins from lysates of RCC10 and RCC63 cells were loaded onto SDS-polyacrylamide gels and immunoblotted with antibodies against IRP1 and IRP2. The latter antibody recognized histidine-tagged rat recombinant IRP2 (*r-IRP2*). When indicated, the cells were exposed to FAC or DFO for 24 h. The blots were reprobed with an antibody against β-actin as a loading control. The result shown is representative of three independent experiments. *B*, Northern blot analysis of IRP2 mRNA: a filter with equal amounts of total RNA (as revealed by the ethidium bromide fluorescence of ribosomal RNA) was hybridized with human IRP2 cDNA. The result shown is representative of two separate experiments. *C*, RNA bandshift analysis of IRP activity and aconitase enzymatic activity. Cytoplasmic extracts were incubated with an excess of a ^{32}P-labeled iron responsive element probe and RNA-protein complexes separated on non-denaturing polyacrylamide gels. For supershift analysis, the extracts were preincubated with an antibody against IRP1 (*α-IRP1*) before binding. The autoradiogram is representative of three independent experiments. Aconitase activity was measured spectrophotometrically as described under "Materials and Methods." *D*, Northern blot analysis of ferritin mRNAs: a filter with equal amounts of total RNA (as revealed by the ethidium bromide fluorescence of ribosomal RNA) was hybridized with human L and H cDNAs. When indicated, the cells were exposed to FAC or DFO for 24 h. The autoradiogram is representative of three independent experiments.

bined activity of both was 1.5 times higher in the RCC cells lacking VHL (Fig. 4*C*, *lanes 1* and *3*). We also performed supershift experiments to determine the contributions of the two IRPs to binding activity in RCC cells. We incubated cytosolic extracts with a saturating amount of the antibody against IRP1 and evaluated the supershifted IRP1 band, whereas the amount of RNA-binding activity that was not supershifted was taken as an indication of IRP2 activity. We found that IRP1 and IRP2 were increased to a similar extent (about 1.5-fold) in the RCC10 cells. In keeping with these findings, aconitase enzymatic activity was 30% less in the RCC10 than in the RCC63 cells (Fig. 4*C*, *bottom*). In both cell lines, the binding activities of IRP1 and IRP2, as well as aconitase activity, were modulated as expected by FAC and DFO (results not shown).

Taken together, the different assays assessing the content and activity of IRPs indicate that RCC10 cells have a slightly smaller LIP than RCC63 cells, thus indicating that the limited activation of IRP2 in RCC10 cells is not directly caused by reduced proteolysis due to the absence of VHL. An additional line of evidence against an important role for abnormal lack of IRP2 degradation, specifically caused by the absence of VHL, in determining the low ferritin expression in RCC10 cells was provided by a Northern blot analysis, which showed that the decrease in ferritin was regulated at mRNA level. Fig. 4*D* shows that the levels of both the H and the L transcripts were considerably lower (70% reduction) in RCC10 cells. Once again, exposure to treatments leading to iron overload or deprivation caused changes in ferritin mRNA levels in both cell lines, but the effects caused by manipulating cellular iron content led to smaller differences in ferritin gene expression than those found between the two untreated cell lines. Altogether, these results showed that the differences in ferritin content between the two cell lines are regulated at multiple

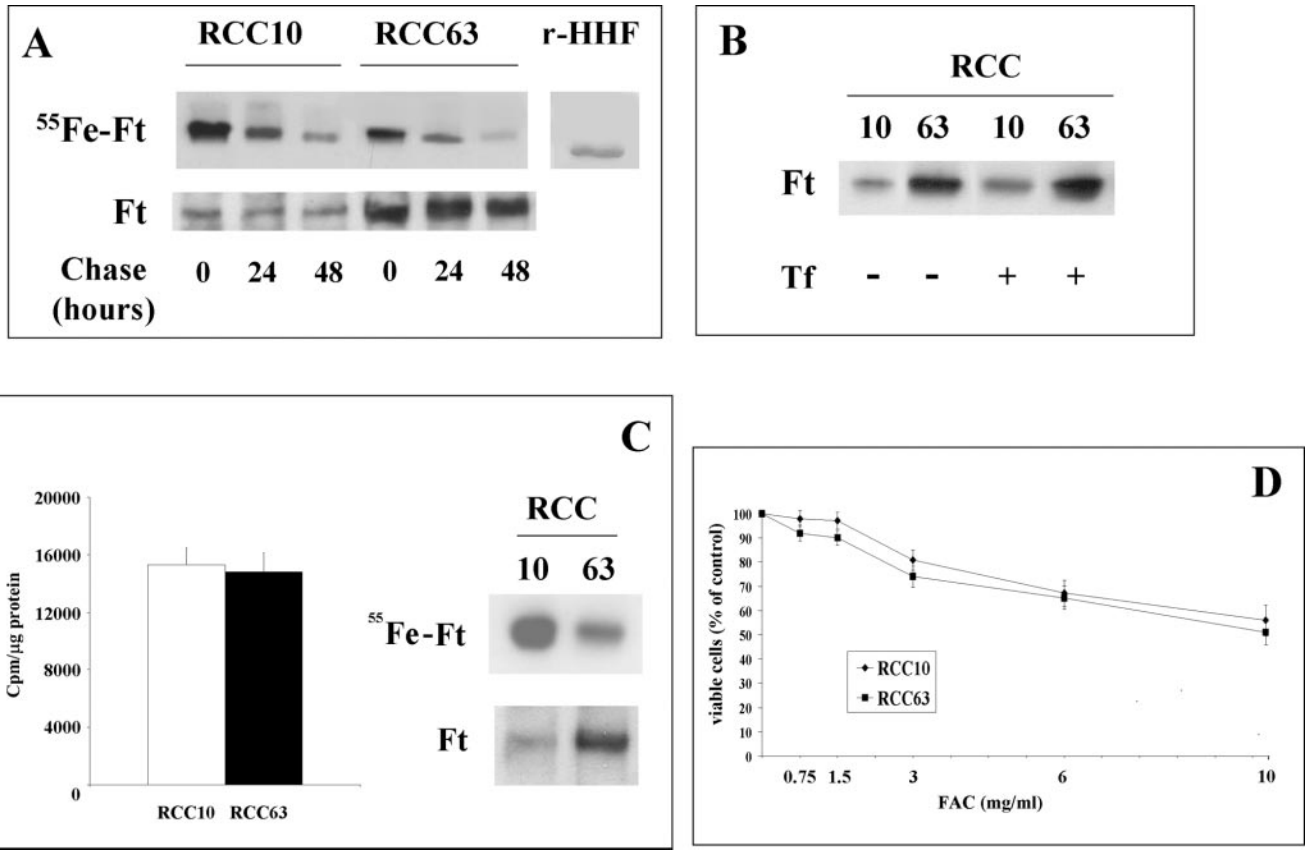

FIG. 5. **Effect of VHL loss on iron trafficking and iron-mediated cytotoxicity.** *A*, ferritin incorporation of Tf-derived ^{55}Fe: RCC cells were incubated for 24 h in the presence of ^{55}Fe-Tf as described in the legend to Fig. 2. Equal amounts of proteins of cell lysates prepared at the end of the labeling period or after a 24- and 48-h chase with unlabeled Tf were analyzed by means of native PAGE. ^{55}Fe-labeled ferritin (^{55}Fe-Ft) was revealed by autoradiography and identified on the basis of the migration of purified recombinant human H chain ferritin (*r-HHF*) run in parallel. The autoradiogram is representative of three separate experiments. Equal amounts of proteins from the same lysates were also loaded onto native polyacrylamide gels and immunoblotted with antibodies against human ferritin H subunit (*Ft*). The results are representative of three experiments. *B*, effect of transferrin on ferritin content. Equal amounts of proteins of cell lysates from RCC cells incubated for 24 h in the presence or in the absence of 1 μM diferric transferrin were loaded onto native polyacrylamide gels and immunoblotted with antibodies against human ferritin H subunit (*Ft*). The results are representative of three experiments. *C*, ^{55}Fe-FAC incorporation. RCC cells were incubated for 24 h in the presence of ^{55}Fe-FAC. The cells were then washed and homogenized as described under "Materials and Methods." Cellular iron uptake (*left*) is expressed as radioactive iron in total homogenates. Mean values ± S.D. of three separate experiments. The cell lysates were also analyzed by means of native PAGE (*right*). ^{55}Fe-labeled (*^{55}Fe-Ft*) or unlabeled (*Ft*) ferritin were revealed by autoradiography or incubation with antibodies against human ferritin H subunit, respectively. The results are representative of three experiments. *D*, effect of VHL on iron-mediated toxicity: RCC10 and RCC63 cells were left untreated or exposed to increasing concentrations of FAC for 24 h. Toxicity was evaluated as the percentage of viable cells measured by MTT assay, an indicator of mitochondrial function. Mean values ± S.D. of five experiments.

levels: in RCC10 cells a reduced amount of ferritin mRNAs and an increase in the binding activity of both IRPs cooperate to repress ferritin expression.

Loss of VHL Affects Iron Trafficking—In an attempt to understand how RCC10 cells, which accumulate a considerable amount of iron over time (see Fig. 1*B*), may also have a slightly reduced LIP, we next determined the fate of the internalized Tf-bound iron. Autoradiography of non-denaturing gels of soluble cell homogenates showed that ferritin accounted for most of the ^{55}Fe-labeled proteins and that the radioactive iron associated with ferritin molecules was about three times greater in the RCC10 cells (Fig. 5*A*). When the cells were subjected to a 24- to 48-h chase with unlabeled Tf to allow intracellular iron redistribution, ferritin labeling decreased, possibly because of ferritin turnover, but, as the extent of the reduction was similar in both cell lines, the ferritin in the RCC10 cells still contained more radioactive iron. In agreement with the enzyme-linked immunosorbent assay results, immunoblot analysis for H ferritin subunit performed using the same radioactive extracts showed a much lower ferritin content in RCC10 than in RCC63 cells. This finding suggests that VHL-deficient cells have an increased capacity to promptly and efficiently store excess iron in ferritin shells. Indeed, incubation in the presence of the same concentration of diferric transferrin (1 μM) used in the iron incorporation experiments did not significantly affect the ferritin content of the two cell lines (Fig. 5*B*).

To understand whether increased Tf-bound iron availability plays a role in determining the results shown in Fig. 5*A*, we exposed the RCC cells to non-transferrin-bound radioactive iron supplied as FAC. In this case, the total cell content of ^{55}Fe iron determined by liquid scintillation counting was not statistically different between the RCC63 and RCC10 cells (Fig. 5*C*), but ferritin-associated radioactivity was more than 2.5-times higher in the RCC10 cells, which had a lower H ferritin subunit content, as shown by immunoblotting (Fig. 5*C*). VHL-deficient cells therefore not only incorporate the iron taken up through the disrupted and up-regulated TfR pathway more efficiently into ferritin but also the iron taken up through the TfR-independent pathway.

The greater ability to store iron in ferritin anticipates that RCC10 cells are more resistant to iron-mediated damage. However, it has been reported that decreasing ferritin levels increases the susceptibility to iron toxicity (27). To assess this point further, we exposed the two RCC cell lines to an iron load. When the cells were treated with increasing concentrations of FAC (Fig. 5*D*), cell viability was slightly but significantly

higher ($p < 0.05$) in RCC10 cells at the lower doses (0.75–3 mg/ml range) and not different at the higher concentrations, probably because at these doses the increased storage capacity of these cells is not sufficient to buffer all the incoming iron. The lack of large differences in cytotoxicity indicates that the more efficient incorporation and/or storage of iron in ferritin only partially compensates for the reduced ferritin content of RCC10 cells.

DISCUSSION

The VHL protein is the substrate-recognition component of a multiprotein ubiquitin ligase complex that binds and targets proteins to polyubiquitination and proteasome-mediated degradation (9). Because the major target of VHL is the transcriptional complex hypoxia inducible factor (HIF-1α), its loss up-regulates hypoxia-inducible genes that facilitate tumor growth in adverse microenvironments and assist the progress of invasion and angiogenesis (10–12). Our results show that, by means of different molecular mechanisms acting at multiple levels, the loss of VHL leads to a profound rearrangement of the expression pattern of the major genes of iron metabolism and intracellular iron handling. A recent study has demonstrated that RCC10 cells are similar to other widely used VHL-defective cell lines in terms of the expression of significant amounts of HIF-1α under normoxic conditions and the absence of detectable HIF-1α upon the restoration of normal VHL function (38). Therefore, it is conceivable that the disruption of iron homeostasis may be a consequence of VHL inactivation. However, only analysis of other independent renal carcinomas and their respective wild type transfectants will provide definitive evidence that the observed effects depend only on VHL loss.

We found that the absence of a functional VHL strongly induces TfR expression and, although a post-transcriptional control exerted by the decrease of the LIP could also play a role (see below), we also provide molecular evidence that this up-regulation is mainly HIF1-mediated at transcriptional level, thus further supporting the role of the HIF-1-related pathway in iron homeostasis (10, 14–16). Importantly, the higher expression of TfR leads to increased iron accumulation.

An unexpected finding was that ferritin expression is down-modulated by the loss of VHL. Under physiological conditions, the increased TfR expression induced by iron deficiency comes to an end once the necessary amount of iron has been introduced, but, in RCC10 cells, TfR expression is constitutively and non-physiologically up-regulated by the loss of VHL, thus leading to a considerable and permanent increase in iron uptake. Surprisingly, the excess iron entering RCC10 cells is accompanied by a remarkable reduction in the expression of ferritin, largely caused by a considerable decrease in the transcripts of both ferritin subunits, particularly the H chain. Studies involving the high throughput analysis of gene expression have shown that VHL can affect the expression of a large number of genes, often independently of HIF-1. In terms of ferritin expression, the results are controversial, because a different response pattern of both the H and L subunits has been characterized in various studies (39–42). These discrepancies underscore the limitations of large-scale gene expression analyses, and may reflect variations in RCC cell lines and the use of different methodologies. It is worth noting that the above studies did not analyze ferritin at protein level, and only one study (40) confirmed the array data by means of a more quantitative assay, whereas we validated our findings at mRNA level by showing remarkable and reproducible changes in ferritin chains at protein level.

In relation to the molecular basis underlying the different levels of ferritin transcripts, although it is clear that HIF-1 cannot be involved in up-modulating ferritin transcription, because the levels of the H and L subunit mRNAs are low in RCC10 cells in which HIF-1 is highly expressed and active (see Figs. 1 and 2), we cannot detail the transcriptional mechanisms underlying the differences in ferritin expression. Small increases in ferritin mRNA levels may be triggered by iron (43, 44), but we believe that the different ferritin expression in the two RCC cell lines is not mediated by iron, because the manipulation of cell iron content that greatly changed the intracellular iron pool (see the IRP analysis, Fig. 4) led to smaller differences in ferritin mRNA levels than those found between the two untreated cell lines (see Fig. 4), whose similar IRP activity indicates that they have comparable LIP levels. Because IRP2 mRNA levels are modulated by iron deficiency (45), the finding that the IRP2 mRNA content in RCC10 and RCC63 cells is similar, whereas that of ferritin mRNA is remarkably different, further suggests that the iron status of the two cell lines is not considerably different and therefore indicates that the different expression of ferritin mRNA is iron-independent.

The different extent of ferritin down-modulation at protein (more than 5-fold) and mRNA level (3-fold) suggests the possible existence of post-transcriptional controls. The 50% increase in IRP-binding activity in VHL-defective cells may facilitate the transcriptionally determined increase in TfR expression and contribute to the decrease in ferritin levels through translational repression. However, the lack of VHL does not seem to act directly through IRP2 stabilization in a way that is similar to its action on HIF-1. In fact, IRP2 is down-modulated by iron also in VHL-defective RCC10 cells, thus demonstrating that VHL is not necessary for IRP2 degradation; moreover, a number of different assays indicated that IRP1 activity is also somewhat greater in RCC10 cells, thus suggesting there is a small decrease in the LIP of this cell line that enhances the binding of both IRPs. These findings showing that VHL is not involved in IRP2 degradation are in agreement with the lack of VHL-dependent ubiquitination of IRP2 by extracts of VHL-defective cells (46) or VBC-Cul2 ligase (47) and with results showing that iron-dependent IRP2 proteolysis is not compromised in VHL-defective cells (48).

Although we cannot rule out the possibility that the small reduction in the LIP of RCC10 cells is a result of their slightly (but not statistically significant) faster growth rate, we think that it is more probably caused by a more efficient sequestration of iron into ferritin. This mechanism, which is possibly facilitated by the shift of the ferritin H/L ratio in favor of the L chain, which is more suitable for storage, leads to a ferritin that is about 20 times richer in iron. An increased accumulation of iron in ferritin has been previously found in anthracycline-treated cells (49) and attributed to an inhibition of mobilization caused by interference with the lysosome/proteasome pathway (50). However, we have previously demonstrated that the anthracycline-induced deposition of iron in ferritin is associated with increased ferritin expression (18), and our pulse-chase experiments (Fig. 5) did not reveal any differences in ferritin iron mobilization. Therefore, we report here a process of more efficient iron sequestration, either facilitated by a cofactor or simply reflecting random distribution of iron in existing, partially loaded, ferritin shells, which may represent a mechanism for safe metal storage in cells with low ferritin content. An increased capacity of ferritin to sequester iron, with a possibly similar protective meaning, has been reported in hydrogen peroxide-treated fibroblasts (51).

The cellular availability of iron, which is a cofactor necessary for HIF hydroxylation, contributes to tuning the physiological response to hypoxia (11). Therefore, the decrease of LIP that we observe in VHL-deficient cells as a result of enhanced iron deposition in ferritin may represent another potentially impor-

tant factor of reduced HIF degradation, eventually contributing to HIF-mediated induction of target genes in cancer cells, which are in turn responsible for angiogenesis, glucose transport and metabolism, cell survival and invasion, among others (10–13).

Myc overexpression, which inversely modulates the transcription of the genes for H ferritin and IRP2, has been interpreted as a means of ensuring transformed cells the availability of more iron for purposes of growth, although this study did not directly explore iron movements (8). Our results showing altered TfR and ferritin expression following the loss of VHL are in line with those of Wu *et al.* (8), insofar as the modulated expression of the genes of iron metabolism can be considered one of the metabolic alterations that both the activation of an oncogene or the loss of a tumor suppressor gene use to give cancer cells selective growth advantages or better adaptation to an adverse environment. However, we also provide evidence that, at least in the case of the loss of VHL, still undefined post-translational mechanisms affecting iron handling by ferritin modify the availability of iron, somehow counteracting the effects caused by the reduced content of this protective protein. Indeed, despite their diminished ferritin content, RCC10 cells do not show any greater sensitivity to damaging insults such as iron overload or oxidative stress. Another consequence of this more efficient iron incorporation into ferritin shells is that VHL-deficient cells have no excess iron available for cell multiplication, which is reflected in the similar growth rate of the two cell lines and may perhaps provide a rationale for the somewhat puzzling common finding that the lack of a functional VHL has little impact on cell multiplication, at least *in vitro* (30).

In conclusion, our results showing that increased amounts of iron enter RCC10 cells as a consequence of the mutation in the VHL gene substantiate previous evidence (8) indicating that iron metabolism is specifically targeted by alterations in genes important for the control of cell growth. However, we have also demonstrated that the excess iron entering RCC10 cells is more efficiently sequestered into ferritin, and hence does not affect proliferation and sensitivity to oxidants. This occurs also with non-transferrin-bound iron (see Fig. 5) and thus represents a novel mechanism for iron storage in cancer cells that may become important under conditions of increased plasma iron levels, which are often found in cancer patients and promoted by chemotherapy (52).

Acknowledgments—We thank Dr. K. Plate (Goethe University, Frankfurt, Germany) for the kind gift of the RCC10 and RCC63 cell lines, Dr. L. Kuhn for the plasmids encoding the TfR promoter and the IRE probe, Dr. E. Leibold for the plasmid coding for IRP2, and Prof. G. Minotti for reading the manuscript and making helpful suggestions.

REFERENCES

1. Hentze, M. W., Muckenthaler, M. U., and Andrews, N. C. (2004) *Cell* **117,** 285–297
2. Le, N. T., and Richardson, D. R. (2002) *Biochim. Biophys. Acta* **1603,** 31–46
3. Cairo, G., Recalcati, S., Pietrangelo, A., and Minotti, G. (2002) *Free Radic. Biol. Med.* **32,** 1237–1243
4. Harrison, P. M., and Arosio, P. (1996) *Biochim. Biophys. Acta* **1275,** 161–203
5. Hentze, M. W., and Kuhn, L. C. (1996) *Proc. Natl. Acad. Sci. U. S. A.* **93,** 8175–8182
6. Cairo, G., and Pietrangelo, A. (2000) *Biochem. J.* **352,** 241–250
7. Kwok, J. C., and Richardson, D. R. (2002) *Crit. Rev. Oncol. Hematol.* **42,** 65–78
8. Wu, K. J., Polack, A., and Dalla-Favera, R. (1999) *Science* **283,** 676–679
9. Kim, W., and Kaelin, W. G., Jr. (2003) *Curr. Opin. Genet. Dev.* **13,** 55–60
10. Harris, A. L. (2002) *Nat. Rev. Cancer* **2,** 38–47
11. Pugh, C. W., and Ratcliffe, P. J. (2003) *Semin. Cancer. Biol.* **13,** 83–89
12. Semenza, G. L. (2003) *Nat. Rev. Cancer* **3,** 721–732
13. Denko, N. C., Fontana, L. A., Hudson, K. M., Sutphin, P. D., Raychaudhuri, S., Altman, R., and Giaccia, A. J. (2003) *Oncogene* **22,** 5907–5914
14. Tacchini, L., Bianchi, L., Bernelli-Zazzera, A., and Cairo, G. (1999) *J. Biol. Chem.* **274,** 24142–24146
15. Lok, C. N., and Ponka, P. (1999) *J. Biol. Chem.* **274,** 24147–24152
16. Bianchi, L., Tacchini, L., and Cairo, G. (1999) *Nucleic Acids Res.* **27,** 4223–4227
17. Krieg, M., Haas, R., Brauch, H., Acker, T., Flamme, I., and Plate, K. H. (2000) *Oncogene* **19,** 5435–5443
18. Corna, G., Santambrogio, P., Minotti, G., and Cairo, G. (2004) *J. Biol. Chem.* **279,** 13738–13745
19. Tacchini, L., Matteucci, E., De Ponti, C., and Desiderio, M. A. (2003) *Exp. Cell Res.* **290,** 391–401
20. Wang, G. L., and Semenza, G. L. (1995) *J. Biol. Chem.* **270,** 1230–1237
21. Cairo, G., Tacchini, L., Pogliaghi, G., Anzon, E., Tomasi, A., and Bernelli-Zazzera, A. (1995) *J. Biol. Chem.* **270,** 700–703
22. Minotti, G., Ronchi, R., Salvatorelli, E., Menna, P., and Cairo, G. (2001) *Cancer Res.* **61,** 8422–8428
23. Campanella, A., Levi, S., Cairo, G., Biasiotto, G., and Arosio, P. (2004) *Biochemistry* **43,** 195–204
24. Pietrangelo, A., Rocchi, E., Casalgrandi, G., Rigo, G., Ferrari, A., Perini, M., Ventura, E., and Cairo, G. (1992) *Gastroenterology* **102,** 802–809
25. Pietrangelo, A., Casalgrandi, G., Quaglino, D., Gualdi, R., Conte, D., Milani, S., Montosi, G., Cesarini, L., Ventura, E., and Cairo, G. (1995) *Gastroenterology* **108,** 208–217
26. Cairo, G., and Lucchini, M. (1993) *Exp. Cell Res.* **206,** 255–260
27. Cozzi, A., Corsi, B., Levi, S., Santambrogio, P., Biasiotto, G., and Arosio, P. (2004) *Blood* **103,** 2377–2383
28. Corsi, B., Cozzi, A., Arosio, P., Drysdale, J., Santambrogio, P., Campanella, A., Biasiotto, G., Albertini, A., and Levi, S. (2002) *J. Biol. Chem.* **277,** 22430–22437
29. Baba, M., Hirai, S., Kawakami, S., Kishida, T., Sakai, N., Kaneko, S., Yao, M., Shuin, T., Kubota, Y., Hosaka, M., and Ohno, S. (2001) *Oncogene* **20,** 2727–2736
30. Ratcliffe, P. J. (2003) *Nat. Cell Biol.* **5,** 7–8
31. Recalcati, S., Taramelli, D., Conte, D., and Cairo, G. (1998) *Blood* **91,** 1059–1066
32. Recalcati, S., Conte, D., and Cairo, G. (1999) *Eur. J. Biochem.* **259,** 304–309
33. Meyron-Holtz, E. G., Ghosh, M. C., Iwai, K., LaVaute, T., Brazzolotto, X., Berger, U. V., Land, W., Ollivierre-Wilson, H., Grinberg, A., Love, P., and Rouault, T. A. (2004) *EMBO J.* **23,** 386–395
34. Semenza, G. L. (2001) *Curr. Opin. Cell Biol.* **13,** 167–171
35. Hanson, E. S., Rawlins, M. L., and Leibold, E. A. (2003) *J. Biol. Chem.* **278,** 40337–40342
36. Wang, J., Chen, G., Muckenthaler, M., Galy, B., Hentze, M. W., and Pantopoulos, K. (2004) *Mol. Cell. Biol.* **24,** 954–965
37. Bonnah, R. A., Muckenthaler, M. U., Carlson, H., Minana, B., Enns, C. A., Hentze, M. W., and So, M. (2004) *Cell. Microbiol.* **6,** 473–484
38. Cuevas, Y., Hernandez-Alcoceba, R., Aragones, J., Naranjo-Suarez, S., Castellanos, M. C., Esteban, M. A., Martin-Puig, S., Landazuri, M. O., and del Peso, L. (2003) *Cancer Res.* **63,** 6877–6884
39. Jiang, Y., Zhang, W., Kondo, K., Klco, J. M., St Martin, T. B., Dufault, M. R., Madden, S. L., Kaelin, W. G., Jr., and Nacht, M. (2003) *Mol. Cancer Res.* **1,** 453–462
40. Wykoff, C. C., Sotiriou, C., Cockman, M. E., Ratcliffe, P. J., Maxwell, P., Liu, E., and Harris, A. L. (2004) *Br. J. Cancer* **90,** 1235–1243
41. Zatyka, M., da Silva, N. F., Clifford, S. C., Morris, M. R., Wiesener, M. S., Eckardt, K. U., Houlston, R. S., Richards, F. M., Latif, F., and Maher, E. R. (2002) *Cancer Res.* **62,** 3803–3811
42. Bluyssen, H. A., Lolkema, M. P., van Beest, M., Boone, M., Snijckers, C. M., Los, M., Gebbink, M. F., Braam, B., Holstege, F. C., Giles, R. H., and Voest, E. E. (2004) *FEBS Lett.* **556,** 137–142
43. Cairo, G., Bardella, L., Schiaffonati, L., Arosio, P., Levi, S., and Bernelli-Zazzera, A. (1985) *Biochem. Biophys. Res. Commun.* **133,** 314–321
44. White, K., and Munro, H. N. (1988) *J. Biol. Chem.* **263,** 8938–8942
45. Guo, B., Brown, F. M., Phillips, J. D., Yu, Y., and Leibold, E. A. (1995) *J. Biol. Chem.* **270,** 16529–16535
46. Cockman, M. E., Masson, N., Mole, D. R., Jaakkola, P., Chang, G. W., Clifford, S. C., Maher, E. R., Pugh, C. W., Ratcliffe, P. J., and Maxwell, P. H. (2000) *J. Biol. Chem.* **275,** 25733–25741
47. Yamanaka, K., Ishikawa, H., Megumi, Y., Tokunaga, F., Kanie, M., Rouault, T. A., Morishima, I., Minato, N., Ishimori, K., and Iwai, K. (2003) *Nat. Cell Biol.* **5,** 336–340
48. Wang, J., and Pantopoulos, K. (2005) *Biochim. Biophys. Acta* **1743,** 79–85
49. Kwok, J. C., and Richardson, D. R. (2003) *Mol. Pharmacol.* **63,** 849–861
50. Kwok, J. C., and Richardson, D. R. (2004) *Mol. Pharmacol.* **65,** 181–195
51. Caltagirone, A., Weiss, G., and Pantopoulos, K. (2001) *J. Biol. Chem.* **276,** 19738–19745
52. Bradley, S. J., Gosriwitana, I., Srichairatanakool, S., Hider, R. C., and Porter, J. B. (1997) *Br. J. Haematol.* **99,** 337–343